



Selenium and stable mercury isotopes provide new insights into mercury toxicokinetics in pilot whales

Miling Li^{a,b,*}, C. Alicia Juang^a, Jessica D. Ewald^{a,c}, Runsheng Yin^d, Bjarni Mikkelsen^e, David P. Krabbenhoft^f, Prentiss H. Balcom^a, Clifton Dassuncao^{a,b}, Elsie M. Sunderland^{a,b}

^a Harvard John A. Paulson School of Engineering and Applied Sciences, Harvard University, Cambridge, MA 02138, United States

^b Department of Environmental Health, Harvard T.H. Chan School of Public Health, Boston, MA 02115, United States

^c Faculty of Agricultural and Environmental Sciences, Macdonald Campus, McGill University Ste-Anne-de-Bellevue, Quebec H9X 3V9, Canada

^d Department of Civil and Environmental Engineering, University of Wisconsin, Madison, WI, United States

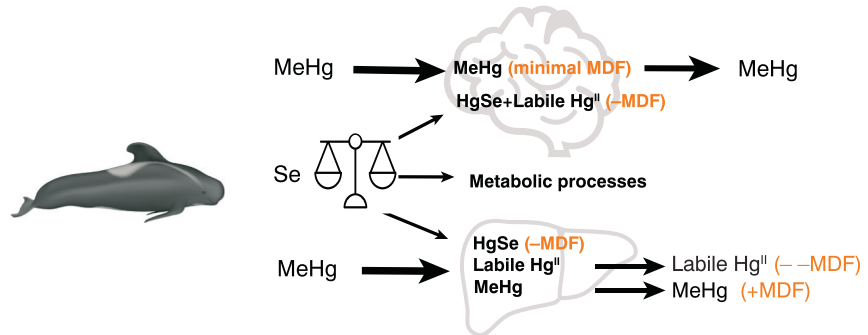
^e The Faroese Museum of Natural History, V. U. Hammershaimsgøta 13, FO-100 Tórshavn, Faroe Islands

^f U.S. Geological Survey, Middleton, WI, USA

HIGHLIGHTS

- The mechanism of Hg metabolism in marine mammals is not fully understood.
- Stable Hg isotopes and Se concentrations in multiple whale tissues were measured.
- The brain $\delta^{202}\text{Hg}$ values are determined by the fraction of Hg present as Hg^{II} .
- We observe variability in $\delta^{202}\text{Hg}$ values in liver tissues across whale life stages.
- Reduced Se availability may drive Hg redistribution among pilot whale tissues.

GRAPHICAL ABSTRACT



ARTICLE INFO

Article history:

Received 15 October 2019

Received in revised form 16 December 2019

Accepted 23 December 2019

Available online 27 December 2019

Editor: Mae Sexauer Gustin

Keywords:

Marine mammals
Ecotoxicology
Bioaccumulation
Methylmercury

ABSTRACT

High exposures of mammalian species to inorganic mercury (Hg^{II}) and methylmercury (MeHg) have been associated with adverse effects on behavior and reproduction. Different mammalian species exhibit varying responses to similar external exposure levels, reflecting potential differences in Hg toxicokinetics. Here, we use Hg stable isotopes, total Hg, MeHg and selenium (Se) concentrations measured in multiple tissues of North Atlantic pilot whales (*Globicephala melas*) to investigate processes affecting the distribution and accumulation of Hg^{II} and MeHg. We find that simple mixing of two distinct isotopic end-members: MeHg (1.4‰) and Hg^{II} (−1.6‰) can explain the observed variability of $\delta^{202}\text{Hg}$ in brain tissue. A similar isotopic composition for the MeHg end-member in the brain, muscle, heart, and kidney suggests efficient exchange of MeHg in blood throughout the body. By contrast, the Hg isotopic composition of the liver of adult whales is different from younger whales and other tissues that follow the two-end member mixing model. Measured Se:Hg ratios are lowest in adult whales with the highest levels of MeHg exposure. In these individuals, Se availability is likely reduced by complexation with demethylated Hg^{II} . We speculate that this results in a higher fraction of labile Hg^{II} eliminated from the liver of adult whales compared to young whales and subsequent redistribution to other tissues, potentially affecting toxicity.

© 2018 Elsevier B.V. All rights reserved.

* Corresponding author at: 111 Robinson Hall, Newark, DE 19716, USA
E-mail address: milingli@udel.edu (M. Li).

1. Introduction

Methylmercury (MeHg) is a potent neurotoxicant that biomagnifies in food webs. Dietary ingestion is the major exposure pathway for MeHg in animals and humans (Hall et al., 1997; Mergler et al., 2007). Many marine mammal populations are exposed to high levels of MeHg, which has been linked to both neurotoxicity and liver lesions (Rawson et al., 1993; Dietz et al., 2013). Large differences in Hg concentrations and speciation have been documented within and among mammalian species (Ostertag et al., 2013). Past studies have reported that total Hg concentrations in brain tissues of fish-eating mammalian species vary by almost six orders of magnitude (Haines et al., 2010b; Krey et al., 2012). In some wildlife (adult polar bears, mink, and otters), Hg in brain tissue is predominantly MeHg (>83% of total Hg) (Basu et al., 2009; Haines et al., 2010b; Krey et al., 2012). By contrast for adult toothed whales and dolphins, Hg in brain tissue is mainly inorganic Hg (Hg^{II} > 75% of total Hg), likely reflecting internal demethylation of MeHg (Huggins et al., 2009; Lemes et al., 2011; Nakazawa et al., 2011). Sensitivity to similar external exposure levels has been reported to differ dramatically among mammalian species. For example, Hg concentrations exceeding $10 \mu\text{g g}^{-1}$ have been measured in the brains of toothed whales, but acute poisoning and death have been reported in humans at only $1\text{--}3 \mu\text{g g}^{-1}$ Hg (Korbass et al., 2010; Dietz et al., 2013). Differences in Hg speciation and concentrations in the brain and sensitivities to exposure are suggestive of variability in Hg transport and metabolism within and across species.

Hg metabolism in mammals is not fully understood. Thiol and selenol-containing biomolecules are believed to play major roles by facilitating transformation and transport of Hg species due to their strong binding affinity for inorganic Hg (Hg^{II}) and MeHg (Wang et al., 2012). Hg^{II} and MeHg complexes with selenols may be more thermodynamically stable than their thiol analogs because selenols are more powerful nucleophiles than thiols (Wang et al., 2012). High levels of inert mercuric selenide nanoparticles HgSe(s) , are commonly found in marine mammal tissues such as the brain and liver, suggesting Se may mediate Hg toxicokinetics (Huggins et al., 2009; Lemes et al., 2011; Nakazawa et al., 2011; Gajdosechova et al., 2016). Laboratory experiments show that selenoamino acids chemically interact with MeHg and eventually convert MeHg to HgSe(s) (Yang et al., 2008; Khan and Wang, 2010). However, HgSe(s) nanoparticles and Se speciation in biological tissues are difficult to accurately quantify due to analytical challenges with solid precipitates (Ewald et al., 2018). Typical measurements of Hg species in marine mammal tissues only include MeHg and total Hg concentrations and thus cannot fully elucidate toxicokinetic processes.

Hg isotopes provide a powerful new tool for investigating Hg sources, biogeochemical processes, and Hg metabolism (Laffont et al., 2011b; Sherman et al., 2013a; Li et al., 2014; Feng et al., 2015; Perrot et al., 2016; Masbou et al., 2018). Both mass-dependent fractionation of Hg isotopes (MDF, reported as $\delta^{202}\text{Hg}$) and mass-independent fractionation (MIF, reported as $\Delta^{199}\text{Hg}$) occur in natural environments. All seven Hg stable isotopes undergo MDF as the result of many physical, chemical, and biological processes (Bergquist and Blum, 2007; Estrade et al., 2009; Kritee et al., 2009; Rodriguez-Gonzalez et al., 2009; Zheng and Hintelmann, 2009; Sherman et al., 2010; Ghosh et al., 2013). MDF has been reported during *in vivo* Hg methylation and demethylation processes when lighter Hg isotopes are preferentially biotransformed (Kritee et al., 2009; Rodriguez-Gonzalez et al., 2009; Janssen et al., 2016). Consistent enrichment of $\delta^{202}\text{Hg}$ (1–2‰) in mammalian muscle and human hair relative to dietary exposure sources has been widely reported and is thought to reflect *in vivo* demethylation of MeHg (Laffont et al., 2011b; Sherman et al., 2013a; Li et al., 2014; Perrot et al., 2016). Batch experiments showed that lighter isotopes of Hg^{II} in solution preferentially bind with thiol groups (Wiederhold et al. 2010). The MDF associated with other Hg toxicokinetic processes such as MeHg-thiol or -selenol formation remains unknown. MIF of the odd-mass-number isotopes (^{199}Hg and ^{201}Hg) occurs predominantly during photochemical

reactions and is thought to be unaffected by dark biological processes, including Hg metabolism (Bergquist and Blum, 2007; Kwon et al., 2012; Perrot et al., 2016).

The main objective of this study was to better understand factors affecting the distribution and accumulation of Hg^{II} and MeHg in mammalian tissues. We hypothesized that speciated Hg accumulation would vary across tissues and life stages of whales and would be associated with Se concentrations. To test this hypothesis, we measured concentrations of total Hg, total Se, MeHg, and Hg stable isotopes in the brain, kidney, liver, heart, and muscle of seven North Atlantic pilot whales (*Globicephala melas*) from a single pod. Pilot whales in the same pod have a high degree of group stability and forage together (Aguilar et al., 1993; Amos et al., 1993; Visser et al., 2014), allowing our study design to minimize Hg isotopic variability originated from dietary MeHg exposure sources (Li et al., 2014).

2. Materials and methods

2.1. Sample collection

Soft tissues (brain, heart, kidney, liver, and muscle) from seven long-finned pilot whales were collected by the Museum of Natural History in the Faroe Islands during the summer of 2016 and were frozen at -20°C . Frozen tissues were subsampled and shipped to Harvard University for analysis, following all ethical protocols for sampling and international conventions for species protection (National Marine Fisheries Service Permit No. 17278-01). We obtained muscle tissues for the primary prey items of pilot whales from the Faroese Marine Research Institute (Desportes and Mouritsen, 1993). Samples included blue whiting (*Micromesistius poutassou*, $n = 7$), oceanic squid (*Todarodes sagittatus*, $n = 7$), and greater argentine (*Argentina silus*, $n = 5$). All tissues were freeze-dried and homogenized before chemical analyses.

2.2. Age determination

We used the length of each whale to estimate their age, following the cetacean growth curve equations for female and male whales based on the Laird/Gompertz model (Bloch et al., 1993). Details of growth equations can be found in the Supporting Information (SI). Pilot whales achieve sexual maturity when body lengths reach 378.8 ± 2.5 cm (mean \pm SD) for females and 493.8 ± 4.6 cm for males (Bloch et al., 1993). We used these length thresholds to categorize whales as juveniles or adults.

2.3. Total Hg, MeHg, and Se analysis

We measured total Hg concentrations in the skeletal muscle, heart, and brain tissues of pilot whales by thermal decomposition, amalgamation, and atomic absorption spectrophotometry (EPA method 7473) using a Nippon MA-3000 Direct Mercury Analyzer (DMA) (U.S. EPA, 2007). To minimize potential carryover issues, the instrument was purged twice between each sample and two blanks were run before sample analysis. Certified reference materials (CRMs: DORM-4 fish protein, DOLT-5 dogfish liver, and PACS-3 marine sediment) were tested every six samples. Average recoveries were 97%, 100%, and 108% for DORM-4 ($n = 1$), DOLT-5 ($n = 8$), and PACS-3 ($n = 8$), respectively. The analytical uncertainty of sample duplicates was $3 \pm 3\%$ (mean \pm SD; $n = 12$). Liver and kidney samples had very high total Hg concentrations that exceeded the calibration range of the instrument. We therefore digested and diluted these samples with DI water before analysis on the DMA. Certified reference materials were prepared and measured in the same way and the average recoveries were 112%, 96%, and 85% for DORM-4 ($n = 2$), DOLT-5 ($n = 1$), and PACS-3 ($n = 2$), respectively. Additional details on methods and QA procedures are provided in the SI.

Methylmercury concentrations in all samples were measured using isotope dilution on a Tekran 2700 MeHg auto-analyzer coupled to a

Thermo iCAP-Q ICP-MS following the methods described in Li et al. (2016). Two certified reference materials (DORM-4 and DOLT-5) were used to check ongoing precision and recovery (OPR) standards every 15 samples. DORM-4 ($n = 2$) and DOLT-5 ($n = 2$) recovery ranged from 96% and 115%, respectively. The analytical uncertainty of sample digestion duplicates was within 4% ($n = 4$).

Total Se concentrations of all tissues were analyzed using methods modified from Evans et al. (2016) and Ashoka et al. (2009). Briefly, we digested samples with 3 mL nitric acid and 1 mL hydrogen peroxide for 24 h at room temperature, heated the digest at 85 °C for 45 min, and diluted samples with deionized water after 24 h. We measured Se concentrations in the samples using a Thermo iCAP-Q ICP-MS in kinetic energy discrimination mode (KED) to minimize interference. Certified reference materials (DORM-4 and DOLT-5) were treated and measured in the same way as samples. The average recoveries were 82% and 88% for DORM-4 ($n = 2$) and DOLT-5 ($n = 2$), respectively. We adjusted the Se concentration of each sample to 100% recovery using an average recovery of 85%, following procedures established in prior studies (Haines et al., 2010a; Evans et al., 2016).

2.4. Mercury stable isotope analysis

Samples were prepared following previously established protocols for processing fish and whale tissues and analyzed using a Neptune Plus multicollector inductively coupled plasma mass spectrometer (MC-ICP-MS) (Laffont et al., 2009; Perrot et al., 2010; Li et al., 2016). Briefly, approximately 0.1–0.2 g of freeze-dried and homogenized samples were digested at 120 °C for 6 h using a 2 mL acid mixture (HCl/HNO₃ = 1:3, v/v) and then were diluted to 1 ng mL⁻¹ for Hg isotope analysis. The sample introduction system and analytical methods for stable Hg isotope analysis follow previous studies (Li et al., 2016; Yin et al., 2016). Data nominations follow the protocols developed by Blum and Bergquist (2007). MDF is expressed using $\delta^{202}\text{Hg}$ notation (Eq. (1)). MIF is expressed as the difference between the measured $\delta^{xxx}\text{Hg}$ value and the value predicted based on MDF and the $\delta^{202}\text{Hg}$ value (Eqs. (2) and (3)) (Blum and Bergquist, 2007).

$$\delta^{202}\text{Hg} = \left[\frac{{}^{202/198}\text{Hg}_{\text{sample}}}{{}^{202/198}\text{Hg}_{\text{NIST3133}}} - 1 \right] \times 10^3\text{‰} \quad (1)$$

$$\Delta^{199}\text{Hg} \approx \delta^{199}\text{Hg} - \left(\delta^{202}\text{Hg} \times 0.2520 \right) \quad (2)$$

$$\Delta^{201}\text{Hg} \approx \delta^{201}\text{Hg} - \left(\delta^{202}\text{Hg} \times 0.7520 \right) \quad (3)$$

CRMs (DORM-4, DOLT-5) were prepared and analyzed in the same way as the samples. The UM-Almadén standard solution (1.0 ng mL⁻¹, diluted in 10% aqua regia) was measured once every 10 samples. The measured Hg isotopic composition of UM-Almadén ($\delta^{202}\text{Hg} = -0.52 \pm 0.03\text{‰}$, $\Delta^{199}\text{Hg} = -0.02 \pm 0.02\text{‰}$, mean \pm SD; $n = 11$) and DORM-4 ($\delta^{202}\text{Hg} = 0.55 \pm 0.02\text{‰}$, $\Delta^{199}\text{Hg} = 1.61 \pm 0.04\text{‰}$, mean \pm SD; $n = 5$) agreed well with prior work (Bergquist and Blum, 2007; Li et al., 2016; Madigan et al., 2018). We measured for the first time the isotope ratios of a dogfish liver standard DOLT-5 ($\delta^{202}\text{Hg} = 0.12 \pm 0.04\text{‰}$ and $\Delta^{199}\text{Hg} = 0.64 \pm 0.05\text{‰}$, mean \pm SD; $n = 5$). Details of the Hg isotopes measured in all CRMs and a comparison with previous DOLT reference material are provided in Table S1.

3. Results and discussion

3.1. Accumulation patterns differ between MeHg and Hg^{II} in whale tissues

Fig. 1 shows MeHg concentrations in all tissues were higher in older individuals up to whales of approximately 10 years of age, after which concentrations appear to plateau (blue symbols, Fig. 1, Table S2). In skeletal muscle and heart tissues, over 90% of the total Hg is present as MeHg. Thus, both total Hg and MeHg show the same pattern in these tissues. By contrast, brain, liver, and kidney tissues from older whales contain a much greater fraction of Hg^{II} (~90% of total Hg) than MeHg. The increase in total Hg concentrations with age reflects continuous accumulation of Hg^{II} in these tissues over their lifetime (Fig. 1 A-C), as has been similarly observed for other marine mammals (Masbou et al., 2015; Masbou et al., 2018).

MeHg is the only Hg species that crosses the blood-brain barrier (Aschner and Aschner, 1990; Bridges and Zalups, 2010). Hg^{II} in the brain is thus a product of demethylated MeHg that is trapped by the blood-brain barrier and accumulates over time as the whales age. Previous work has suggested that in the brain of toothed whales and dolphins, MeHg is continuously demethylated to Hg^{II} and subsequently immobilized by formation of Se nanoparticles (HgSe(s)), resulting in Hg^{II} accumulation (Huggins et al., 2009; Lemes et al., 2011; Nakazawa et al., 2011; Gajdosechova et al., 2016). Our results are consistent with this explanation. In older whales, measured Hg^{II} concentrations in the

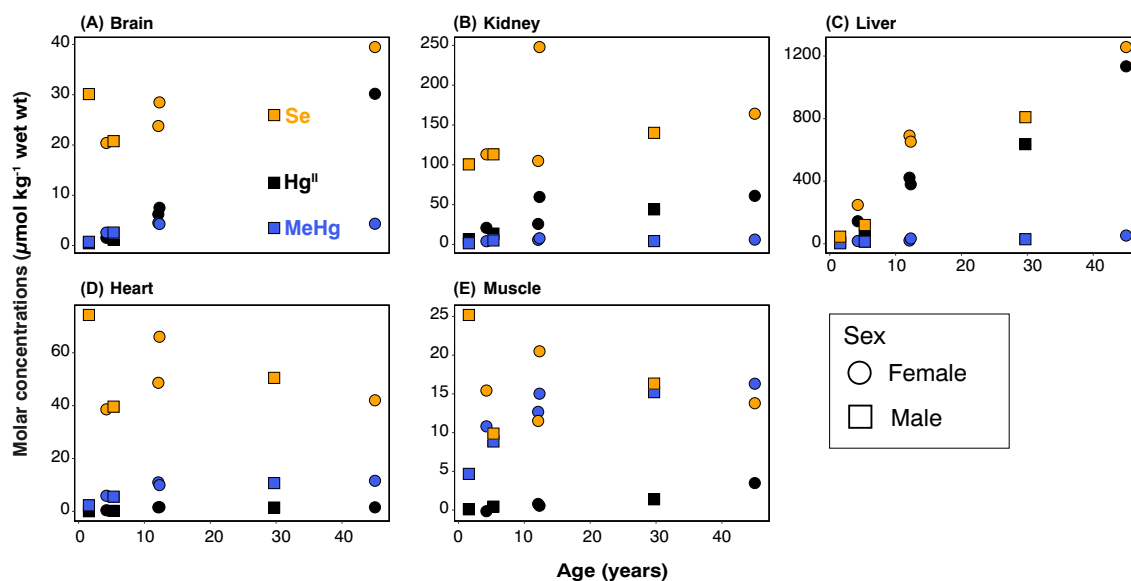


Fig. 1. Concentrations of methylmercury (blue, MeHg), inorganic Hg (black, Hg^{II}) calculated by subtracting MeHg from measured total Hg, total selenium (orange, Se) in pilot whale tissues. Squares indicate males and circles indicate females. (For interpretation of the references to colour in this figure legend, the reader is referred to the web version of this article.)

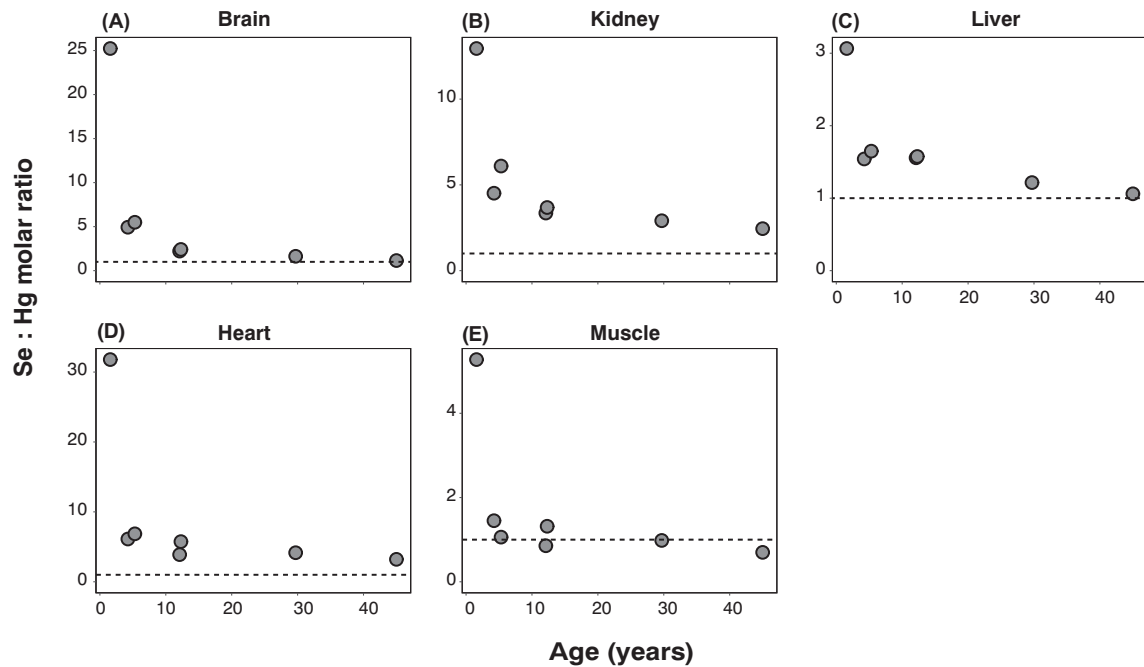


Fig. 2. Se:Hg molar ratios measured in tissues of pilot whales with different ages. The dashed line indicates equal Se:Hg molar ratio.

liver were up to 19 times higher than those in the kidney and brain. The liver is the primary organ responsible for producing selenoproteins in mammals (Gladyshev, 2011). Our results suggest the liver is also the dominant tissue where Hg^{II} is immobilized by formation of Se nanoparticles.

3.2. Selenium distribution across tissues varies by life stages

Measured concentrations of Se vary across whale tissues and life stages and are significantly correlated with Hg^{II} concentrations in the liver ($r = 1.0$, $p < 0.001$) and kidney ($r = 0.8$, $p < 0.05$) but not in other tissues (Fig. 1, orange symbols). MeHg is weakly correlated with Se concentrations in all tissues except the liver ($r = 0.9$, $p < .05$). In liver tissues, Se and Hg^{II} concentrations both increased with individual age. In the liver of older whales, Se concentrations were up to 30-times higher than the youngest whales (Fig. 1C). In brain and kidney tissues, Se showed much smaller increases with age (~2 times) relative to liver tissues (Fig. 1A&B). Extremely high concentrations of both Hg^{II} and Se were observed in the kidney of one adult whale 12 years of age (Fig. 1B). Total Hg in heart and muscle tissues consisted predominantly of MeHg. Se concentrations measured in these tissues did not increase in older whales (Fig. 1D&E). Higher Se concentrations in heart tissue relative to muscle may result from a greater volume of circulating blood carrying selenoproteins (Gladyshev, 2011). Among tissues, measured Se concentrations were the highest in the liver except for the youngest whale (<2 years) that had the highest concentrations in the kidney (Fig. S1). This is consistent with prior work on Hg in ringed seals that showed preferential partitioning of Hg^{II} into the kidney of juvenile ringed seals compared to adult seals (Ewald et al., 2018). Our results further suggest that Se plays a role in partitioning of Hg species among tissues in marine mammals.

Selenium-to-mercury (Se:Hg) molar ratios for all tissues were highest in the youngest whales aged 2–5 years and approached unity (1:1) in all organs in older whales (Fig. 2). The difference between molar concentrations of Se and Hg varied across tissues and life stages (Fig. S2). In brain tissue, the difference between molar concentrations of Se and Hg gradually declined from 29 $\mu\text{mol}/\text{kg}$ in the 2-year-old whale to 5 $\mu\text{mol}/\text{kg}$ in a 45-year-old whale (Fig. S2A). Liver tissues show a sharp increase in Se compared to Hg concentrations in young

whales between ages 2 and 10 years. In liver tissue from individuals over 10 years of age, the difference between molar concentrations of Se and Hg rapidly declined (Fig. S2B). In kidney tissues, the difference between molar concentrations of Se and Hg appears to remain at approximately 100 $\mu\text{mol}/\text{kg}$ across all individual ages in this study (Fig. S2C).

3.3. Metabolic processes lead to variability in Hg isotopes

The $\Delta^{199}\text{Hg}$ values measured in pilot whale muscle tissues in this study ($1.12 \pm 0.14\%$) fall within the range of their common prey items (Desportes and Mouritsen, 1993) from the same geographic region: oceanic squid ($1.18 \pm 0.12\%$), greater argentine ($1.28 \pm 0.04\%$), blue whiting ($0.93 \pm 0.10\%$) (Fig. 3). Fractionation of $\Delta^{199}\text{Hg}$

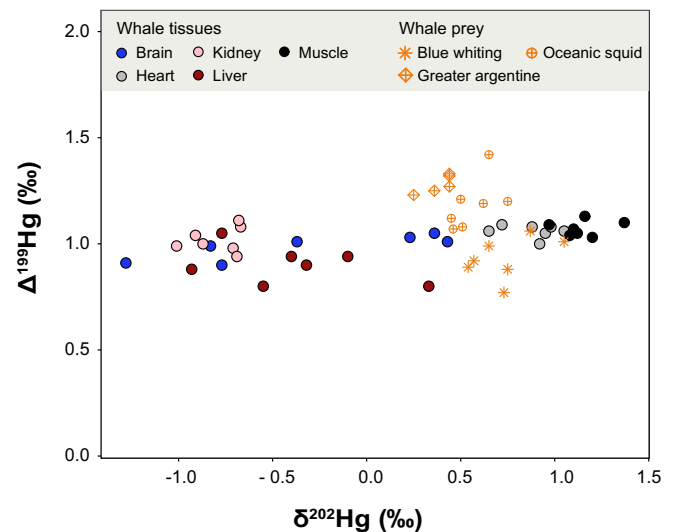


Fig. 3. Stable Hg isotopes ($\Delta^{199}\text{Hg}$ and $\delta^{202}\text{Hg}$) measured in pilot whale tissues and typical prey items (oceanic squid, blue whiting, and greater argentine). (For interpretation of the references to colour in this figure legend, the reader is referred to the web version of this article.)

has been established as a good proxy for the foraging depth in oceanic fish (Blum et al., 2013). Prior work shows the range of $\Delta^{199}\text{Hg}$ measured in fish ranges between 0 and 6‰. In this study, $\Delta^{199}\text{Hg}$ values in whale tissues and their common prey items are on the low end of the published literature range. This suggests pilot whales forage at depths where the accumulated MeHg has not undergone substantial photodegradation prior to being taken up in the marine food web (Bergquist and Blum, 2007). We found low variability in $\Delta^{199}\text{Hg}$ (range: 0.80 to 1.13‰) across tissues and whales in this study, which confirms the similarity in dietary sources of MeHg across whales in mesopelagic waters (200–500 m) and the absence of *in vivo* MIF during digestion and metabolism, as supported by previous work (Desportes and Mouritsen, 1993; Rodriguez-Gonzalez et al., 2009; Laffont et al., 2011a; Kwon et al., 2012; Sherman et al., 2013b; Li et al., 2014; National Oceanic and Atmospheric Administration, 2019).

We measured large differences in $\delta^{202}\text{Hg}$ among pilot whale tissues (~2.6‰) (Fig. 4). All tissue-specific $\delta^{202}\text{Hg}$ values are positively correlated with the fraction of Hg present as MeHg, except in the liver (Fig. 4). Pilot whales obtain MeHg from dietary exposure. It is well established that >90% of the total Hg in predatory fish, including the primary prey (squid, blue whiting, and other fish) of pilot whales, is present as MeHg (Bloom, 1992; Storelli et al., 2003; Bustamante et al., 2006). After dietary MeHg is absorbed in gastrointestinal tract, it quickly enters the bloodstream and a large portion is transported to the liver where demethylation occurs (Bridges and Zalups, 2005; Khan and Wang, 2009). The residual MeHg that has not been demethylated can be reabsorbed in the gallbladder and intestinal tract and eventually circulate back to the bloodstream (Clarkson and Magos, 2006). MeHg stored in muscle is the residual MeHg excreted from the liver following *in vivo* demethylation (Perrot et al., 2016).

The depleted $\delta^{202}\text{Hg}$ signature of Hg^{II} measured here in both the kidney and the liver is consistent with preferential demethylation of MeHg containing lighter Hg isotopes in these tissues. This results in a residual MeHg pool with enriched $\delta^{202}\text{Hg}$ values (Fig. 4). Enriched $\delta^{202}\text{Hg}$ signatures in the brain, heart, and muscle are consistent with transport of enriched $\delta^{202}\text{Hg}$ in MeHg from the liver, through the bloodstream and into other tissues.

Previous work has reported a consistent positive MDF of Hg between muscle tissues of mammalian predators and their prey, which has been attributed to metabolic processes in mammals (Laffont et al., 2011a; Perrot et al., 2012; Sherman et al., 2013b; Li et al., 2014; Perrot et al.,

2016). The muscle tissues of pilot whales in this study are enriched by an average of 0.55‰ $\delta^{202}\text{Hg}$ compared to prey species (Fig. 3). This is lower than the previously reported MDFs between seals and their prey (~1‰) and between human hair and seafood (~2‰) (Laffont et al., 2011a; Perrot et al., 2012; Sherman et al., 2013b; Li et al., 2014). Hg isotope ratios in whale prey items are variable (range: 0.25–1.05‰). However, this is insufficient for explaining the much larger MDF observed between human hair and seafood. We hypothesize that the smaller MDF observed between whales and their prey compared to humans reflects more metabolic and toxicokinetic pathway (s) for MeHg in humans such as partitioning of Hg between blood and hair and demethylation in hair follicles (Berglund et al., 2005; Clarkson and Magos, 2006).

3.4. Toxicokinetics of MeHg in the brain

Brain tissues of juvenile whales in this study had higher %MeHg and enriched $\delta^{202}\text{Hg}$ values compared to adults (Fig. 4). We find a strong linear correlation between $\delta^{202}\text{Hg}$ in the brain and %MeHg ($R^2 = 0.94$, $p < 0.01$). This indicates variability in $\delta^{202}\text{Hg}$ can be described by the simple mixing of two distinct end-members: MeHg (1.4‰) and Hg^{II} (−1.6‰) (Fig. 4). The Hg^{II} end-member found in the brain must represent all Hg^{II} species present in the brain because neither labile Hg^{II} nor HgSe(s) can cross the blood-brain-barrier (Aschner and Aschner, 1990; Bridges and Zalups, 2010). The approximately 3.0‰ difference in $\delta^{202}\text{Hg}$ between MeHg and Hg^{II} in the brain is similar to the previously reported ~3.0‰ enrichment in MeHg relative to Hg^{II} for seal tissues (Perrot et al., 2016). Consistency in these values across marine mammals suggests a similar toxicokinetic mechanism for MeHg demethylation across species.

The $\delta^{202}\text{Hg}$ values for the MeHg end-member in the brain align well with those from muscle and heart tissues, indicating a similar source of MeHg with constant $\delta^{202}\text{Hg}$ values to all organs (Fig. 4). Bolea-Fernandez et al. (2019) reported consistent $\delta^{202}\text{Hg}$ values (0.96–1.27‰) in blood samples of pilot whales, similar to that of the MeHg end-member in this study and higher than the $\delta^{202}\text{Hg}$ values of total Hg in all other tissues (e.g., muscle, heart, liver, kidney). Efficient exchange of MeHg between the bloodstream and various tissues (Clarkson et al., 2007), including the brain, appears to homogenize the Hg isotopic composition of MeHg end-member in tissues throughout the whale body.

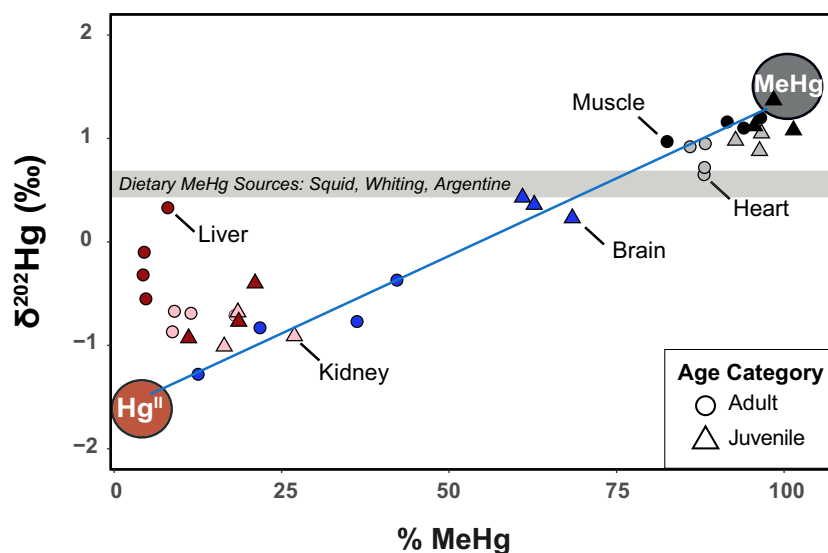


Fig. 4. Relationship between $\delta^{202}\text{Hg}$ values across and within pilot whale tissues and the fraction of total Hg present as methylmercury (%MeHg) in different whale tissues. Brain tissue data were used to develop the regression line shown in the figure (solid blue line; $\delta^{202}\text{Hg} = -1.6 + 0.03(\% \text{MeHg})$, $R^2 = 0.94$, $p < 0.001$). The grey shaded region shows the Hg isotope composition (mean \pm 1 SD) of typical whale prey items (oceanic squid, blue whiting, and greater argentine). (For interpretation of the references to colour in this figure legend, the reader is referred to the web version of this article.)

3.5. Toxicokinetics of MeHg differ across life stages

Among liver tissues, we observed much larger inter-individual variability in $\delta^{202}\text{Hg}$ values (1.4%, ranging from -0.9 to 0.3%) compared to muscle, heart, and kidney tissues ($<0.5\%$). In the liver of juvenile whales, $\delta^{202}\text{Hg}$ values decreased with greater total Hg concentrations but the opposite pattern was observed in three out of four adults, where $\delta^{202}\text{Hg}$ values increased with greater total Hg concentrations. These differences suggest variability in $\delta^{202}\text{Hg}$ values across life stages may be controlled by different mechanisms (Fig. 5A). Similar patterns in isotopic composition across life stages have been observed in other studies of pilot whales and beluga whales (Masbou et al., 2018; Bolea-Fernandez et al., 2019).

We observed a decline in both $\delta^{202}\text{Hg}$ values and %MeHg in the liver of juvenile whales with increasing Hg exposures (Fig. 5A and Fig. S3). This likely reflects preferential demethylation of MeHg with lighter Hg isotopes that results in more Hg^{II} with lower $\delta^{202}\text{Hg}$ values in the liver. Prior work in pilot whales hypothesized that dietary shifts during weaning may also lead to a depletion in $\delta^{202}\text{Hg}$ values in the liver (Bolea-Fernandez et al., 2019). During the weaning period for pilot whales (<7 years for males and <12 years for females) milk is gradually replaced with small fish and squid (Desportes and Mouritsen, 1993). Our data suggest this dietary transition would push $\delta^{202}\text{Hg}$ values in the opposite direction because $\delta^{202}\text{Hg}$ values in pilot whale milk samples (0.14%; Bolea-Fernandez et al. (2019)) are lower than those in common pilot whale prey measured here (range: 0.25–1.05%). Therefore, we do not think the lower $\delta^{202}\text{Hg}$ values observed in juvenile individuals with increasing Hg exposures as a function of age in this study can be explained by dietary shifts during weaning.

For adult whales in this study, $\delta^{202}\text{Hg}$ values in the liver increased in older individuals. This is unlikely to reflect different dietary exposure sources because all whales in this study were from the same pod and thus encountered similar dietary sources of MeHg (Visser et al., 2014). Similarity in adult whale dietary MeHg exposure is supported by their consistent $\Delta^{199}\text{Hg}$ values (Fig. 3). Almost all of the total Hg (96–98%) measured in the liver of adult pilot whales consists of Hg^{II} species (Fig. 5A). Thus, small differences in the fraction of MeHg should exert

little influence on liver $\delta^{202}\text{Hg}$ values. We therefore posit that preferential export of Hg^{II} with lower $\delta^{202}\text{Hg}$ values to other organs is the most plausible explanation for enriched $\delta^{202}\text{Hg}$ values of total Hg in this tissue. Feng et al. (2015) observed a similar progressive enrichment in heavier Hg isotopes in the liver of laboratory fish caused by redistribution of Hg^{II} from the liver to other organs.

Since $\text{HgSe}(s)$ is inert (Wang et al., 2012), a different Hg^{II} species that is labile must be transported out of the liver in adult whales following demethylation. Wang et al. (2012) suggest this labile Hg^{II} form consists of Hg thiolic complexes $\text{Hg}(\text{SR})_2$ (e.g., Hg-cysteinates). Bolea-Fernandez et al. (2019) found that $\text{HgSe}(s)$ particles are enriched in heavier Hg isotopes (i.e., higher $\delta^{202}\text{Hg}$) compared to labile Hg^{II} in pilot whale liver. Preferential export of labile $\text{Hg}(\text{SR})_2$ with lower $\delta^{202}\text{Hg}$ values relative to $\text{HgSe}(s)$ from the liver would leave a residual pool of Hg in the liver of older whales with enriched $\delta^{202}\text{Hg}$ values and could explain the observed increasing $\delta^{202}\text{Hg}$ values in older whales (Fig. 5A). Such a change in the Hg^{II} composition of whale liver is consistent with prior work showing increases in the bound:labile Hg^{II} ratios and the number of HgSe nanoparticles with age (Gajdosechova et al., 2016).

3.6. New insights into the role of Se in Hg metabolism

Seleno-containing biomolecules are known to initiate or aid in MeHg demethylation, leading to $\text{HgSe}(s)$ formation in various tissues (Khan and Wang, 2010; Wang et al., 2012; Zayas et al., 2014). Besides binding and immobilizing Hg, Se is required for biosynthesis of essential amino acids and enzymes (Gromer et al., 2005; Ralston and Raymond, 2010). Therefore, Se in excess of the molar ratio of Hg present in tissues is likely needed to support essential metabolic processes in biological tissues. Only specific seleno biomolecules such as Se-cysteine directly participate in MeHg demethylation and $\text{HgSe}(s)$ formation. Prior work has shown that extensive MeHg detoxification could deplete the biological pool of Se (Se-methionine) needed to maintain Se-cysteine levels in the brain and liver of pilot whales (Gajdosechova et al., 2016). Reduced Se availability can lead to a variety of adverse health outcomes, including reduced coordination, autoimmune disorders, and increased susceptibility to infectious diseases (Hoffmann and Berry, 2008; Shahar et al., 2010).

Results of this study suggest that both Se and Hg affect the distribution of Hg among pilot whale tissues. For adult whales in this study, we observed an increase in $\delta^{202}\text{Hg}$ values in liver tissue from older individuals and a concomitant decrease in the difference between molar concentrations of Se and Hg (Fig. 5A&B). Seleno-containing biomolecules bind Hg^{II} therefore a reduced difference between molar concentrations of Se and Hg may limit the pool of Se available for other metabolic processes. We speculate that lower differences between the molar concentrations of Se and Hg in older whales with high Hg concentrations may inhibit further sequestration of labile Hg^{II} as $\text{HgSe}(s)$ in the liver. This could facilitate preferential circulation of labile Hg^{II} depleted in $\delta^{202}\text{Hg}$ out of the liver, which is consistent with higher $\delta^{202}\text{Hg}$ values in older pilot whales.

Kidney tissues of adult pilot whales contain high fractions of total Hg as Hg^{II} but the difference between molar concentrations of Se and Hg is fairly stable across individuals and ages (Fig. S4). There may thus be sufficient Se in the kidney to immobilize the Hg^{II} , limiting loss of labile Hg^{II} from this tissue in older whales. This could explain why kidney tissues of adult whales do not become isotopically heavier with age like the liver, as observed in this study and in Bolea-Fernandez et al. (2019). Future work on establishing the essential metabolic level of tissue-specific Se concentrations will further improve our understanding of how Se affects the metabolism and distribution of Hg species.

4. Conclusion

Prior work indicates that MeHg demethylation may increase toxicity at specific target sites by producing reactive Hg^{II} that leads to oxidative stress, inhibits neuron receptors, and depletes Se required for other essential biological functions (Basu et al., 2006; Shapiro and Chan, 2008;

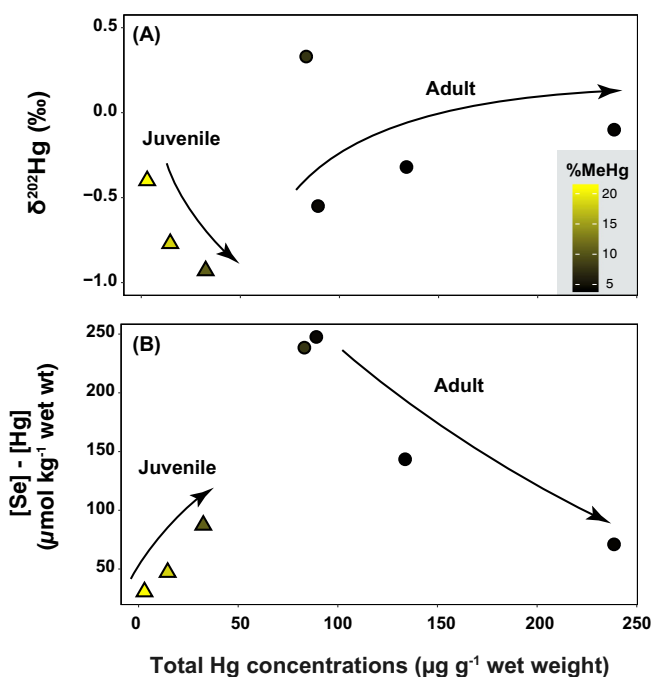


Fig. 5. Variability of (A) $\delta^{202}\text{Hg}$ values and (B) the difference between molar concentrations of Se and Hg in the liver as a function of total Hg concentrations. The colour bar represents the %MeHg in liver tissues.

Gajdosechova et al., 2016). Measurements of stable Hg isotopes and Hg species in multiple tissues of pilot whales from a single pod across a range of ages collected in this study suggest continuous *in vivo* demethylation occurs in the brain, liver, and kidney. Accumulation of Hg^{II} continues even after MeHg concentrations stabilize, raising concerns associated with Hg^{II} toxicity.

Our study links Hg toxicokinetic processes implied by Hg isotope data with Se measurements in tissues and suggests that Se availability may drive Hg redistribution among tissues. In whale brain tissue, we found a strong linear relationship between $\delta^{202}\text{Hg}$ values and the fraction of total Hg present as MeHg that can be described by mixing of two distinct isotopic end-members (Hg^{II}: -1.6% and MeHg: 1.4%). The $\delta^{202}\text{Hg}$ value of the MeHg end-member is similar to other tissues that contain predominantly MeHg (heart, muscle). These results are consistent with continuous production and accumulation of demethylated Hg^{II} with depleted $\delta^{202}\text{Hg}$ in the brain and efficient exchange of MeHg between the brain and bloodstream.

In liver tissues, we identified contrasting trends in $\delta^{202}\text{Hg}$ values with age in juvenile and adult whales, suggesting Hg toxicokinetic mechanisms may differ across life stages. We hypothesize that reduced Se availability in whales with higher total Hg in their liver may lead to a greater fraction of labile Hg^{II} being circulated out of the liver of adult whales and into other organs. Intra and inter-species differences in Hg speciation and sensitivity to Hg exposures are well documented but the understanding of underlying causes is still limited. Results from this study suggest the combined information from Hg stable isotopes and Se can help decipher Hg toxicokinetic processes and shed light on interactions between different Se and Hg species.

Declaration of competing interest

All authors declare no competing financial interest.

Acknowledgments

We thank Høgni Arnbjarnarson (Faroese Museum of Natural History) for assistance with samples and Niladri Basu (McGill University) for comments on an earlier draft of this manuscript. Any use of trade, product, or firm names in this publication are for descriptive purposes only and does not imply endorsement by the U.S. Government.

Funding

This work was supported by the Harvard National Institute of Environmental Health Sciences (NIEHS) Center Grant (P30 ES000002), the National Science Foundation-National Institutes of Environmental Health Sciences Oceans and Human Health Program (OCE-1321612), and the USGS Toxics Hydrology Program.

Appendix A. Supplementary data

Additional explanatory text related to methods and figures and one table are available in the Supporting Information. Data collected in this study are included in a separate spreadsheet. Supplementary data to this article can be found online at doi:<https://doi.org/10.1016/j.scitotenv.2019.136325>.

References

Aguilar, A., Jover, L., Borrell, A., 1993. Heterogeneities in organochlorine profiles of Faroese long-finned pilot whales: indication of segregation between pods. Report of the International Whaling Commission 14, 359–367.

Amos, B., Bloch, D., Desportes, G., Majerus, T., Bancroft, D., Barrett, J., Dover, G., 1993. A review of the molecular evidence relating to social organisation and breeding system in the long-finned pilot whale. Report of the International Whaling Commission 14, 209–217.

Aschner, M., Aschner, J.L., 1990. Mercury neurotoxicity: mechanisms of blood-brain barrier transport. *Neurosci. Biobehav. Rev.* 14, 169–176.

Ashoka, S., Peake, B.M., Bremner, G., Hageman, K.J., Reid, M.R., 2009. Comparison of digestion methods for ICP-MS determination of trace elements in fish tissues. *Anal. Chim. Acta* 653, 191–199.

Basu, N., Scheuhammer, A.M., Rouvinen-Watt, K., Grochowina, N., Klenavik, K., Evans, R.D., Chan, H.M., 2006. Methylmercury impairs components of the cholinergic system in captive mink (*Mustela vison*). *Toxicol. Sci.* 91, 202–209.

Basu, N., Scheuhammer, A.M., Sonne, C., Letcher, R.J., Born, E.W., Dietz, R., 2009. Is dietary mercury of neurotoxicological concern to wild polar bears (*Ursus maritimus*)? *Environ. Toxicol. Chem.* 28, 133–140.

Berglund, M., Lind, B., Björnberg, K.A., Palm, B., Einarsson, Ö., Vahter, M., 2005. Inter-individual variations of human mercury exposure biomarkers: a cross-sectional assessment. *Environ. Health* 4, 20.

Bergquist, B.A., Blum, J.D., 2007. Mass-dependent and -independent fractionation of Hg isotopes by photoreduction in aquatic systems. *Science* 318, 417–420.

Bloch, D., Lockyer, C., Zachariassen, M., 1993. Age and growth parameters of the long-finned pilot whale off the Faroe Islands. *Rep. Int. Whaling Comm. Spec.* 163–207.

Bloom, N.S., 1992. On the chemical form of mercury in edible fish and marine invertebrate tissue. *Can. J. Fish. Aquat. Sci.* 49, 1010–1017.

Blum, J.D., Bergquist, B.A., 2007. Reporting of variations in the natural isotopic composition of mercury. *Anal. Bioanal. Chem.* 388, 353–359.

Blum, J.D., Popp, B.N., Drazen, J.C., Choy, C.A., Johnson, M.W., 2013. Methylmercury production below the mixed layer in the North Pacific Ocean. *Nat. Geosci.* 6, 879–884.

Bolea-Fernandez, E., Rua-Ibarz, A., Krupp, E.M., Feldmann, J., Vanhaecke, F., 2019. High-precision isotopic analysis sheds new light on mercury metabolism in long-finned pilot whales (*Globicephala melas*). *Sci. Rep.* 9, 7262.

Bridges, C.C., Zalups, R.K., 2005. Molecular and ionic mimicry and the transport of toxic metals. *Toxicol. Appl. Pharmacol.* 204, 274–308.

Bridges, C.C., Zalups, R.K., 2010. Transport of inorganic mercury and methylmercury in target tissues and organs. *Journal of Toxicology and Environmental Health, Part B* 13, 385–410.

Bustamante, P., Lahaye, V., Durnez, C., Churlaud, C., Caurant, F., 2006. Total and organic Hg concentrations in cephalopods from the north eastern Atlantic waters: influence of geographical origin and feeding ecology. *Sci. Total Environ.* 368, 585–596.

Clarkson, T.W., Magos, L., 2006. The toxicology of mercury and its chemical compounds. *Crit. Rev. Toxicol.* 36, 609–662.

Clarkson, T.W., Vyas, J.B., Ballatori, N., 2007. Mechanisms of mercury disposition in the body. *Am. J. Ind. Med.* 50, 757–764.

Desportes, G., Mouritsen, R., 1993. Preliminary results on the diet of long-finned pilot whales off the Faroe Islands. Report of the International Whaling Commission 14 (Special Issue), 305–324.

Dietz, R., Sonne, C., Basu, N., Braune, B., O'Hara, T., Letcher, R.J., Scheuhammer, T., Andersen, M., Andreasen, C., Andriashek, D., 2013. What are the toxicological effects of mercury in Arctic biota? *Sci. Total Environ.* 443, 775–790.

Estrade, N., Carignan, J., Sonke, J.E., Donard, O.F., 2009. Mercury isotope fractionation during liquid–vapor evaporation experiments. *Geochim. Cosmochim. Acta* 73, 2693–2711.

Evans, R., Grochowina, N., Basu, N., O'Connor, E., Hickie, B., Rouvinen-Watt, K., Evans, H., Chan, H., 2016. Uptake of selenium and mercury by captive mink: results of a controlled feeding experiment. *Chemosphere* 144, 1582–1588.

Ewald, J.D., Kirk, J.L., Li, M., Sunderland, E.M., 2018. Organ-specific differences in mercury speciation and accumulation across ringed seal (*Phoca hispida*) life stages. *Sci. Total Environ.* 650, 2013–2020.

Feng, C., Pedrero, Z., Gentès, S., Barre, J., Renedo, M., Tessier, E., Beraïl, S., Maury-Brachet, R., Mesmer-Dudons, N., Baudrimont, M., 2015. Specific pathways of dietary methylmercury and inorganic mercury determined by mercury speciation and isotopic composition in zebrafish (*Danio rerio*). *Environmental science & technology* 49, 12984–12993.

Gajdosechova, Z., Lawan, M.M., Urgast, D.S., Raab, A., Scheckel, K.G., Lombi, E., Kopittke, P.M., Loeschner, K., Larsen, E.H., Woods, G., 2016. *In vivo* formation of natural Hg₂Se nanoparticles in the liver and brain of pilot whales. *Sci. Rep.* 6, 34361.

Ghosh, S., Schauble, E.A., Couloume, G.L., Blum, J.D., Bergquist, B.A., 2013. Estimation of nuclear volume dependent fractionation of mercury isotopes in equilibrium liquid–vapor evaporation experiments. *Chem. Geol.* 336, 5–12.

Gladyshev, V.N., 2011. Selenoproteins and selenoproteomes. *SeleniumSpringer*, pp. 109–123.

Gromer, S., Eubel, J., Lee, B., Jacob, J., 2005. Human selenoproteins at a glance. *Cellular and Molecular Life Sciences CMLS* 62, 2414–2437.

Haines, K.J., Evans, R.D., O'Brien, M., Evans, H.E., 2010a. Accumulation of mercury and selenium in the brain of river otters (*Lontra canadensis*) and wild mink (*Mustela vison*) from Nova Scotia, Canada. *Sci. Total Environ.* 408, 537–542.

Haines, K.J., Evans, R.D., O'Brien, M., Evans, H.E., 2010b. Accumulation of mercury and selenium in the brain of river otters (*Lontra canadensis*) and wild mink (*Mustela vison*) from Nova Scotia, Canada. *Sci. Total Environ.* 408, 537–542.

Hall, B., Bodaly, R., Fudge, R., Rudd, J., Rosenberg, D., 1997. Food as the Dominant Pathway of Methylmercury Uptake by Fish. *Water, Air, and Soil Pollution*. 100 pp. 13–24.

Hoffmann, P.R., Berry, M.J., 2008. The influence of selenium on immune responses. *Mol. Nutr. Food Res.* 52, 1273–1280.

Huggins, F.E., Raverty, S.A., Nielsen, O.S., Sharp, N.E., Robertson, J.D., Ralston, N.V., 2009. An XAFS investigation of mercury and selenium in beluga whale tissues. *Environ. Bioindic.* 4, 291–302.

Janssen, S.E., Schaefer, J.K., Barkay, T., Reinfelder, J.R., 2016. Fractionation of mercury stable isotopes during microbial methylmercury production by iron- and sulfate-reducing bacteria. *Environmental science & technology* 50, 8077–8083.

Khan, M.A., Wang, F., 2009. Mercury-selenium compounds and their toxicological significance: toward a molecular understanding of the mercury-selenium antagonism. *Environmental Toxicology and Chemistry: An International Journal* 28, 1567–1577.

- Khan, M.A., Wang, F., 2010. Chemical demethylation of methylmercury by selenoamino acids. *Chem. Res. Toxicol.* 23, 1202–1206.
- Korbas, M., O'Donoghue, J.L., Watson, G.E., Pickering, I.J., Singh, S.P., Myers, G.J., Clarkson, T.W., George, G.N., 2010. The chemical nature of mercury in human brain following poisoning or environmental exposure. *ACS Chem. Neurosci.* 1, 810–818.
- Krey, A., Kwan, M., Chan, H.M., 2012. Mercury speciation in brain tissue of polar bears (*Ursus maritimus*) from the Canadian Arctic. *Environ. Res.* 114, 24–30.
- Kritee, K., Barkay, T., Blum, J.D., 2009. Mass dependent stable isotope fractionation of mercury during *mer* mediated microbial degradation of monomethylmercury. *Geochim. Cosmochim. Acta* 73, 1285–1296.
- Kwon, S.Y., Blum, J.D., Carvan, M.J., Basu, N., Head, J.A., Madenjian, C.P., David, S.R., 2012. Absence of fractionation of mercury isotopes during trophic transfer of methylmercury to freshwater fish in captivity. *Environmental science & technology* 46, 7527–7534.
- Laffont, L., Sonke, J.E., Maurice, L., Hintelmann, H., Pouilly, M., Sanchez Bacarreza, Y., Perez, T., Behra, P., 2009. Anomalous mercury isotopic compositions of fish and human hair in the Bolivian Amazon. *Environmental science & technology* 43, 8985–8990.
- Laffont, L., Sonke, J.E., Maurice, L., Monrroy, S.L., Chincheros, J., Amouroux, D., Behra, P., 2011a. Hg speciation and stable isotope signatures in human hair as a tracer for dietary and occupational exposure to mercury. *Environ. Sci. Technol.* 45, 9910–9916.
- Laffont, L., Sonke, J.E., Maurice, L., Monrroy, S.L., Chincheros, J., Amouroux, D., Behra, P., 2011b. Hg speciation and stable isotope signatures in human hair as a tracer for dietary and occupational exposure to mercury. *Environmental science & technology* 45, 9910–9916.
- Lemes, M., Wang, F., Stern, G., Ostertag, S., Chan, H., 2011. Methylmercury and Selenium Speciation in Different Tissues of Beluga Whales (*Delphinapterus leucas*) from the Western Canadian Arctic. *Environmental toxicology and chemistry/SETAC*.
- Li, M., Sherman, L.S., Blum, J.D., Grandjean, P., Mikkelsen, B., Weihe, P., Sunderland, E.M., Shine, J.P., 2014. Assessing sources of human methylmercury exposure using stable mercury isotopes. *Environmental science & technology* 48, 8800–8806.
- Li, M., Schartup, A.T., Valberg, A.P., Ewald, J.D., Krabbenhoft, D.P., Yin, R., Balcom, P.H., Sunderland, E.M., 2016. Environmental origins of Methylmercury accumulated in subarctic estuarine fish indicated by mercury stable isotopes. *Environmental science & technology* 50, 11559–11568.
- Madigan, D.J., Li, M., Yin, R., Baumann, H., Snodgrass, O.E., Dewar, H., Krabbenhoft, D.P., Baumann, Z., Fisher, N.S., Balcom, P.H., Sunderland, E.M., 2018. Mercury stable isotopes reveal influence of foraging depth on mercury concentrations and growth in Pacific bluefin tuna. *Environmental science & technology* 52 (11), 6256–6264.
- Masbou, J., Point, D., Sonke, J.E., Frappart, F., Perrot, V., Amouroux, D., Richard, P., Becker, P.R., 2015. Hg stable isotope time trend in ringed seals registers decreasing sea ice cover in the Alaskan Arctic. *Environmental science & technology* 49, 8977–8985.
- Masbou, J., Sonke, J.E., Amouroux, D., Guillou, G., Becker, P.R., Point, D., 2018. Hg-stable isotope variations in marine top predators of the western Arctic ocean. *ACS Earth and Space Chemistry* 2, 479–490.
- Mergler, D., Anderson, H.A., Chan, L.H.M., Mahaffey, K.R., Murray, M., Sakamoto, M., Stern, A.H., 2007. Methylmercury exposure and health effects in humans: a worldwide concern. *AMBIO: a Journal of the Human Environment* 36, 3–11.
- Nakazawa, E., Ikemoto, T., Hokura, A., Terada, Y., Kunito, T., Tanabe, S., Nakai, I., 2011. The presence of mercury selenide in various tissues of the striped dolphin: evidence from mu-XRF-XRD and XAFS analyses. *Metallomics* 3, 719–725.
- National Oceanic and Atmospheric Administration, 2019. Long-Finned Pilot Whale. Fisheries.
- Ostertag, S.K., Stern, G.A., Wang, F.Y., Lemes, M., Chan, H.M., 2013. Mercury distribution and speciation in different brain regions of beluga whales (*Delphinapterus leucas*). *Sci. Total Environ.* 456, 278–286.
- Perrot, V., Epov, V.N., Pastukhov, M.V., Grebenshchikova, V.I., Zouiten, C., Sonke, J.E., Husted, S., Donard, O.F.X., Amouroux, D., 2010. Tracing sources and bioaccumulation of mercury in fish of Lake Baikal—Angara River using hg isotopic composition. *Environmental science & technology* 44, 8030–8037.
- Perrot, V., Pastukhov, M.V., Epov, V.N., Husted, S., Donard, O.F., Amouroux, D., 2012. Higher mass-independent isotope fractionation of methylmercury in the pelagic food web of Lake Baikal (Russia). *Environmental science & technology* 46, 5902–5911.
- Perrot, V., Masbou, J., Pastukhov, M.V., Epov, V.N., Point, D., Bérail, S., Becker, P.R., Sonke, J.E., Amouroux, D., 2016. Natural Hg isotopic composition of different Hg compounds in mammal tissues as a proxy for in vivo breakdown of toxic methylmercury. *Metallomics* 8, 170–178.
- Ralston, N.V., Raymond, L.J., 2010. Dietary selenium's protective effects against methylmercury toxicity. *Toxicology* 278, 112–123.
- Rawson, A., Patton, G., Hofmann, S., Pietra, G., Johns, L., 1993. Liver abnormalities associated with chronic mercury accumulation in stranded atlantic bottlenosed dolphins. *Ecotoxicol. Environ. Saf.* 25, 41–47.
- Rodriguez-Gonzalez, P., Epov, V.N., Bridou, R., Tessier, E., Guyoneaud, R., Monperrus, M., Amouroux, D., 2009. Species-specific stable isotope fractionation of mercury during hg(II) methylation by an anaerobic bacteria (*Desulfobulbus propionicus*) under dark conditions. *Environmental science & technology* 43, 9183–9188.
- Shahar, A., Patel, K.V., Semba, R.D., Bandinelli, S., Shahar, D.R., Ferrucci, L., Guralnik, J.M., 2010. Plasma selenium is positively related to performance in neurological tasks assessing coordination and motor speed. *Mov. Disord.* 25, 1909–1915.
- Shapiro, A.M., Chan, H.M., 2008. Characterization of demethylation of methylmercury in cultured astrocytes. *Chemosphere* 74, 112–118.
- Sherman, L.S., Blum, J.D., Johnson, K.P., Keeler, G.J., Barres, J.A., Douglas, T.A., 2010. Mass-independent fractionation of mercury isotopes in Arctic snow driven by sunlight. *Nat. Geosci.* 3, 173–177.
- Sherman, L.S., Blum, J.D., Franzblau, A., Basu, N., 2013a. New insight into biomarkers of human mercury exposure using naturally occurring mercury stable isotopes. *Environmental science & technology* 47, 3403–3409.
- Sherman, L.S., Blum, J.D., Franzblau, A., Basu, N., 2013b. New insight into biomarkers of human mercury exposure using naturally occurring mercury stable isotopes. *Environmental science & technology* 47, 3403–3409.
- Storelli, M., Stuffer, R.G., Storelli, A., Marcotrigiano, G., 2003. Total mercury and methylmercury content in edible fish from the Mediterranean Sea. *J. Food Prot.* 66, 300–303.
- U.S. EPA, 2007. Method 7473: Mercury in Solids and Solutions by Thermal Decomposition, Amalgamation, and Atomic Absorption Spectrophotometry. E. P. A, Washington DC: U.S.
- Visser, F., Miller, P.J., Antunes, R.N., Oudejans, M.G., Mackenzie, M.L., Aoki, K., Lam, F.-P.A., Kvadsheim, P.H., Huisman, J., Tyack, P.L., 2014. The social context of individual foraging behaviour in long-finned pilot whales (*Globicephala melas*). *Behaviour* 151, 1453–1477.
- Wang, F., Lemes, M., Khan, M., 2012. Metallomics of mercury: role of thiol- and selenol-containing biomolecules. *Environmental Chemistry and Toxicology of Mercury* 517.
- Yang, D.-Y., Chen, Y.-W., Gunn, J.M., Belzile, N., 2008. Selenium and mercury in organisms: interactions and mechanisms. *Environ. Rev.* 16, 71–92.
- Yin, R., Krabbenhoft, D., Bergquist, B.A., Wang, Z., Lepak, R.F., Hurley, J.P., 2016. Effects of mercury and thallium concentrations on high precision determination of mercury isotope composition by Neptune plus multiple collector inductively coupled plasma mass spectrometry. *J. Anal. At. Spectrom.* 31 (10), 2060–2068.
- Zayas, Z.P., Ouerdane, L., Mounicou, S., Lobinski, R., Monperrus, M., Amouroux, D., 2014. Hemoglobin as a major binding protein for methylmercury in white-sided dolphin liver. *Anal. Bioanal. Chem.* 406, 1121–1129.
- Zheng, W., Hintelmann, H., 2009. Mercury isotope fractionation during photoreduction in natural water is controlled by its Hg/DOC ratio. *Geochim. Cosmochim. Acta* 73, 6704–6715.